JCB Article

The AP-1A and AP-1B clathrin adaptor complexes define biochemically and functionally distinct membrane domains

Heike Fölsch,[2] Marc Pypaert,[1] Sandra Maday,[1] Laurence Pelletier,[1] and Ira Mellman[1]

[1]Department of Cell Biology, Ludwig Institute for Cancer Research, Yale University School of Medicine, New Haven, CT 06520
[2]Department of Biochemistry, Molecular Biology, and Cell Biology, Northwestern University, Evanston, IL 60208

Most epithelial cells contain two AP-1 clathrin adaptor complexes. AP-1A is ubiquitously expressed and involved in transport between the TGN and endosomes. AP-1B is expressed only in epithelia and mediates the polarized targeting of membrane proteins to the basolateral surface. Both AP-1 complexes are heterotetramers and differ only in their 50-kD μ1A or μ1B subunits. Here, we show that AP-1A and AP-1B, together with their respective cargoes, define physically and functionally distinct membrane domains in the perinuclear region. Expression of AP-1B (but not AP-1A) enhanced the recruitment of at least two subunits of the exocyst complex (Sec8 and Exo70) required for basolateral transport. By immunofluorescence and cell fractionation, the exocyst subunits were found to selectively associate with AP-1B–containing membranes that were both distinct from AP-1A–positive TGN elements and more closely apposed to transferrin receptor–positive recycling endosomes. Thus, despite the similarity of the two AP-1 complexes, AP-1A and AP-1B exhibit great specificity for endosomal transport versus cell polarity.

Introduction

Newly synthesized glycoproteins destined for transport to the plasma membrane or to the endosomal–lysosomal system travel together through the ER and the Golgi complex only to be sorted from each other upon exit from the TGN (Mellman and Warren, 2000). In polarized epithelial cells, another layer of complexity is added to this scheme due to the fact that they maintain distinct apical and basolateral plasma membrane domains (Drubin and Nelson, 1996; Yeaman et al., 1999). Apical and basolateral proteins in a number of epithelial cell types are sorted upon exit from the TGN, but sorting can also occur in endosomes after endocytosis from the cell surface (Keller and Simons, 1997; Mellman and Warren, 2000).

Membrane protein sorting at the TGN and in the endocytic pathway is controlled by specific cytoplasmic domain-targeting determinants (Matter and Mellman, 1994; Marks et al., 1997; Mostov et al., 1999). These determinants contain critical tyrosine or dileucine residues that are often decoded by cytosolic heterotetrameric complexes of the clathrin adaptor protein family (Bonifacino and Dell'Angelica, 1999). Adaptor protein complexes contain two large (~100 kD), one medium (~50 kD), and one small (~20 kD) subunit. There are four major species, AP-1 through AP-4, with AP-1, AP-3, and presumably AP-4 acting at the level of the TGN or endosomes, and AP-2 acting at the plasma membrane (Hirst and Robinson, 1998; Brodsky et al., 2001). Sorting from the TGN to endosomes is also facilitated by a second family of adaptors, the GGA proteins, which interact with nontyrosine motifs (Robinson and Bonifacino, 2001).

Recently, it has become clear that two AP-1 adaptor complexes exist; a ubiquitously expressed AP-1A complex and an epithelial cell–specific complex designated AP-1B. Although AP-1A is required for sorting events between the TGN and endosomes, maybe in cooperation with GGA adaptors (Doray et al., 2002), AP-1B functions in the polarized transport of membrane proteins to the basolateral surface of epithelial cells. The role of AP-1B first became evident from the study of μ1B-deficient LLC-PK1 kidney cells, in which proteins containing basolateral-targeting signals normally interacting with AP-1B are missorted to the apical surface. This "mutant" phenotype could be com-

The online version of this article includes supplemental material.

Address correspondence to Heike Fölsch, Department of Biochemistry, Molecular Biology, and Cell Biology, Northwestern University, 2205 Tech Drive, Evanston, IL 60208-3500. Tel.: (847) 491-5089. Fax: (847) 467-1380. email: h-folsch@northwestern.edu

Key words: epithelial cells; basolateral sorting; exocytosis; TGN; exocyst

Abbreviations used in this paper: CHC, clathrin heavy chain; CI-MPR, cation-independent mannose 6-phosphate receptor; Tfn, transferrin; VSVG, vesicular stomatitis virus G protein.

pletely corrected by the transfection of μ1B cDNA (Fölsch et al., 1999). AP-1A and AP-1B differ only in the identity of their μ1 subunits, μ1A or μ1B, respectively (Fölsch et al., 1999). The expression of μ1B is restricted to epithelial cells and tissues with the exception of liver (Ohno et al., 1999). Although μ1B and μ1A are coexpressed in all μ1B-positive epithelial cells, the AP-1A and AP-1B complexes appear to have largely nonoverlapping functions. The LLC-PK1 phenotype demonstrated that μ1A cannot support basolateral targeting in the absence of μ1B. Conversely, AP-1B cannot support the correct localization of AP-1A cargo to the TGN in μ1A-deficient cells (Fölsch et al., 2001).

The fact that AP-1A and AP-1B adaptor complexes are functionally distinct is remarkable given that they differ by only a single, highly homologous subunit. Thus, it is unclear how the two complexes can sequester their cargo molecules with such selectivity, or how the resulting transport carriers are targeted to such distinct destinations. Here, we provide new information that helps to clarify these issues. Our work suggests that AP-1A and AP-1B define distinct (as opposed to hybrid) populations of clathrin coats and coated membranes involved in lysosomal or basolateral transport, respectively. Furthermore, AP-1B appears to couple polarized sorting to the recruitment of cytosolic components, in particular proteins associated with the mammalian exocyst complex (Guo et al., 2000), thought to play a role in targeting basolateral transport vesicles to the basolateral plasma membrane domain (Grindstaff et al., 1998).

Results

AP-1A and AP-1B localize to different post-Golgi compartments

Previously, we demonstrated that μ1 subunits internally tagged with the HA epitope were incorporated into functional AP-1 complexes. Analysis of LLC-PK1 cell lines stably expressing HA-tagged μ1A or μ1B suggested that both AP-1A and AP-1B were localized to the TGN and to recycling endosomes. This was based on immunofluorescence data showing a colocalization of both complexes with γ-adaptin and transferrin (Tfn). However, both complexes showed different degrees of colocalization with the TGN marker furin; although AP-1A showed some overlap, AP-1B did not (Fölsch et al., 2001).

Therefore, we characterized the distribution of AP-1 complexes with additional markers for the TGN, namely the TGN "resident" protein TGN38 and a temperature-sensitive mutant of the vesicular stomatitis virus G protein (VSVG-ts045). These two proteins also served as presumptive markers for the AP-1A and AP-1B pathways, respectively. The cytoplasmic tail of TGN38 has been shown to interact with μ1A (Ohno et al., 1995), suggesting its transport between the TGN and endosomes is at least partly dependent on AP-1A. Basolateral delivery of VSVG in MDCK cells is dependent on a critical tyrosine, suggesting that its transport involves AP-1B (see next paragraph; Thomas et al., 1993). VSVG-ts045 can be selectively accumulated in the Golgi complex and TGN by shifting expressing cells from 39°C (at which temperature VSVG-ts045 cannot exit the ER) to 20°C for 1–2 h (Scales et al., 1997). Brief incubations at 31°C then allow VSVG-ts045 to leave the Golgi complex and the TGN.

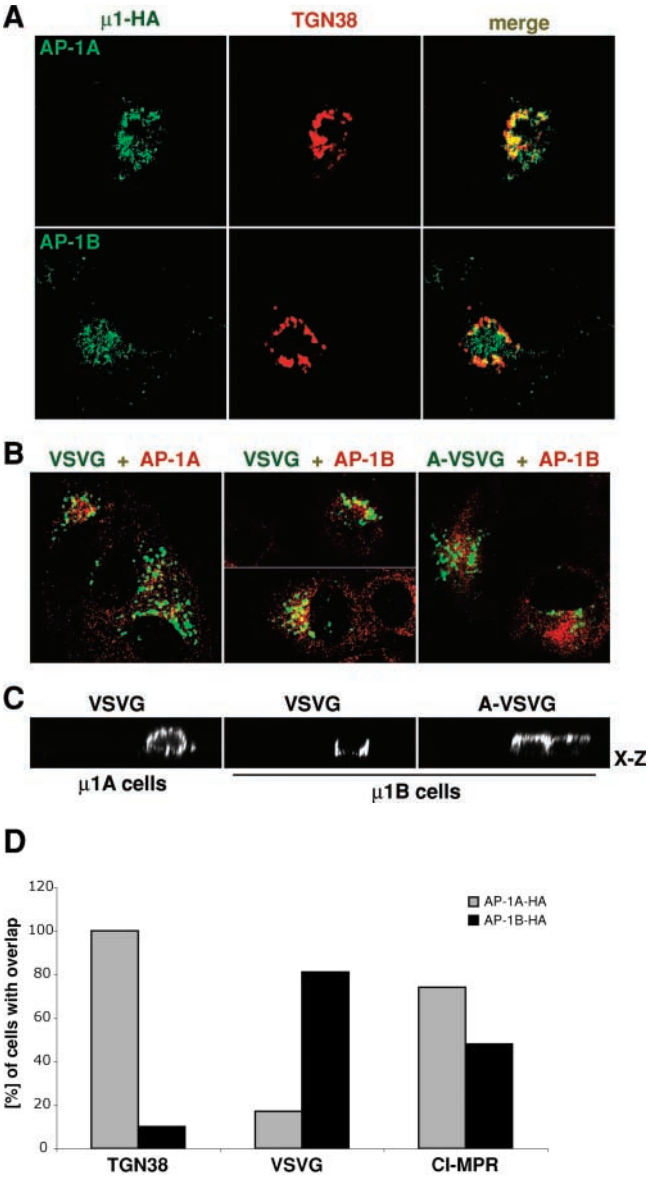

Figure 1. **AP-1A and AP-1B colocalize with their respective cargoes.** (A) LLC-PK1 cells stably transfected with μ1A-HA or μ1B-HA were transiently transfected with cDNAs encoding TGN38. 24 h after transfection, cells were fixed and stained with anti-TGN38 (red) and anti-HA (green). (B) LLC-PK1::μ1A-HA or LLC-PK1::μ1B-HA were microinjected with cDNAs encoding either VSVG-GFP or an apical mutant A-VSVG-GFP. Cells were incubated at 39°C followed by incubation at 20°C. Subsequently, cells were incubated at 31°C for 10 min. Cells were fixed and stained with anti-HA (red). Note that in the case of VSVG expression in AP-1B cells, microinjected cells from two different fields were taken. (C) LLC-PK1::μ1A or μ1B cells were grown on polycarbonate filters for 4 d, microinjected with cDNAs encoding VSVG or A-VSVG, and incubated at 31°C. Surface appearance was monitored by incubating cells with anti-VSVG antibodies before fixation followed by incubation with Alexa® 594–labeled secondary antibodies. (A–C) Specimens were analyzed by confocal microscopy and representative images are shown. (D) Cells from three independent experiments were scored for at least partial overlapping staining. Cells that showed overlapping staining are expressed as percentage of the total number of cells analyzed.

We first monitored the distribution of TGN38 relative to AP-1A and AP-1B by transiently transfecting TGN38 cDNA into LLC-PK1 cell lines stably expressing HA-tagged

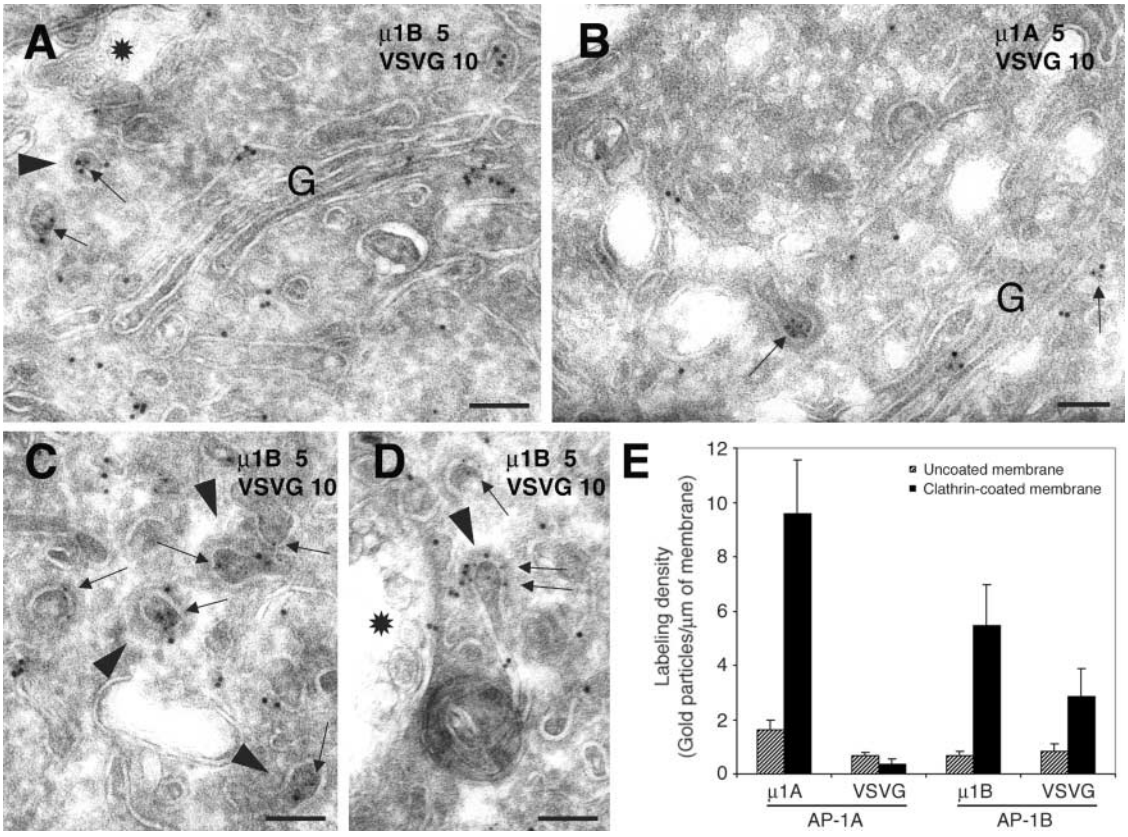

Figure 2. **VSVG colocalizes with AP-1B in clathrin-coated vesicles and buds.** (A–D) LLC-PK1::μ1A-HA (B) or LLC-PK1::μ1B-HA (A, C, and D) were infected with defective adenoviruses encoding VSVG as described in Fig. 1 and analyzed by immuno-EM (see Materials and methods). Small arrows denote labeling for μ1A or μ1B (5-nm gold) on clathrin-coated buds and vesicles. Large arrowheads point to coated buds and vesicles doubly labeled for μ1B and VSVG (A, C, and D). Asterisks, multivesicular endosomes; G, Golgi apparatus. Bars, 100 nm. (E) The labeling density for μ1A/B and VSVG was estimated in AP-1A– and AP-1B–expressing cells as described in Materials and methods. Results are expressed as number of gold particles per length of membrane in μm. Each result is the mean average from three labeling experiments ± SEM.

μ1A or μ1B. As shown in Fig. 1 A, TGN38 (red) colocalized extensively with AP-1A in virtually all transfected cells (green) (Fig. 1 A, top panels; Fig. 1 D). In contrast, TGN38 exhibited a pattern almost entirely distinct from AP-1B, and only 10% of the cells expressing both markers showed any colocalization (Fig. 1 A, bottom panels; Fig. 1 D). These data are in agreement with our previous observations using furin as a TGN marker (Fölsch et al., 2001).

This pattern was different in cells expressing VSVG-ts045 accumulated in the Golgi at 20°C for 2 h then released at 31°C for 10 min. Although VSVG (green) failed in ∼85% of all injected cells to colocalize with AP-1A (Fig. 1 B, left panel; Fig. 1 D), there was at least a regional codistribution of VSVG with AP-1B under the same conditions in ∼80% of the cells (Fig. 1 B, middle; Fig. 1 D). Importantly, a mutant of the VSVG-ts045 that localizes to the apical surface of MDCK cells (Toomre et al., 1999) exhibited little if any overlap with AP-1B (Fig. 1 B, right).

To confirm that VSVG-ts045 depends on AP-1B for basolateral sorting, VSVG cDNAs were microinjected into LLC-PK1 cells stably expressing transfected μ1A or μ1B. Fig. 1 C shows confocal cross sections through cells expressing VSVG-ts045 at the plasma membrane. Although its distribution was nonpolarized in LLC-PK1::μ1A cells (left), VSVG-ts045 was largely basolateral in LLC-PK1::μ1B cells (middle). Basolateral polarity in μ1B expressing cells was diminished with the apical VSVG-ts045 mutant (A-VSVG, right).

Finally, we compared the staining patterns of AP-1A or AP-1B with the cation-independent mannose 6-phosphate receptor (CI-MPR). The CI-MPR has been implicated to interact with both AP-1A and AP-1B complexes (Eskelinen et al., 2002). As shown in Fig. 1 D, there is hardly any difference in the degree of regional overlapping staining between AP-1A or AP-1B complexes and CI-MPR. AP-1A showed at least partial overlapping staining in ∼75% of the cells, and the overlap of AP-1B and CI-MPR was only slightly less (∼50%, Fig. 1 D; Fig. S1, available at http://www.jcb.org/cgi/content/full/jcb.200309020/DC1). These data extend our earlier observation that AP-1A and AP-1B preferentially colocalize with their respective cargo molecules in the perinuclear region.

VSVG accumulates in AP-1B–containing clathrin-coated structures

Because clathrin-coated vesicles are evanescent structures, it is highly unlikely that the overall distribution of AP-1B cargo such as VSVG-ts045 will precisely reflect the overall distribution of AP-1B. As a result, we next determined the distribution of VSVG-ts045 relative to AP-1A– and AP-1B–containing clathrin-coated structures by quantitative immuno-EM. For this purpose, LLC-PK1 cells stably expressing

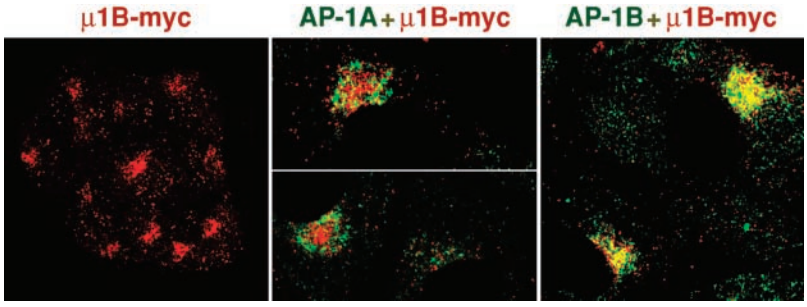

Figure 3. **AP-1A and AP-1B do not colocalize.** (A) LLC-PK1::μ1A-HA or μ1B-HA cells seeded on coverslips were infected with a defective adenovirus encoding μ1B-myc. Subsequently, cells were fixed and stained with anti-myc (red) and anti-HA (green). Specimens were analyzed by confocal microscopy, and representative images are shown. The left panel shows a cluster of cells only stained for μ1B-myc to demonstrate the TGN localization of AP-1B–myc.

HA-tagged μ1A or μ1B were infected with a recombinant adenovirus encoding myc-tagged VSVG-ts045. The various proteins were then localized relative to morphologically identifiable clathrin coats in or around the Golgi region after the temperature shift protocol described earlier in this paper.

Representative images of the localization of μ1A or μ1B and VSVG are shown in Fig. 2. Although labeling for both AP-1A–HA or AP-1B–HA could be found on clathrin-coated buds and vesicles in and around the Golgi complex in the respective cell lines, significant labeling for VSVG in clathrin-coated structures was only observed in AP-1B–expressing cells (Fig. 2, A and B). This observation was confirmed by stereology (Fig. 2 E). Although labeling density for both μ1A-HA and μ1B-HA was significantly higher on clathrin-coated membranes as compared with uncoated membranes, the labeling density for VSVG only increased on clathrin-coated membranes when AP-1B was expressed, and actually showed a decrease in cells without AP-1B. Interestingly, >75% of the clathrin-coated vesicles labeled for VSVG in AP-1B cells were found outside the Golgi region, at a distance of at least 500 nm from any Golgi cisternae and often in proximity to putative endosomal structures (Fig. 2, C and D). Thus, VSVG-ts045 was found to selectively accumulate in AP-1B–positive clathrin-coated structures, particularly those found somewhat outside the region most closely apposed to Golgi cisternae.

AP-1A and AP-1B show nonoverlapping staining patterns

To directly compare the distribution of AP-1A and AP-1B, we infected LLC-PK1 cells stably expressing μ1A-HA or μ1B-HA with a defective adenovirus encoding μ1B with an internal myc tag. The myc tag in μ1B-myc was placed at the same position at which we had successfully placed the HA tag before (Fölsch et al., 2001).

As shown in Fig. 3, μ1B-myc localized to an area of the perinuclear region distinct from AP-1A. In contrast, μ1B-myc showed a significant overlap with AP-1B. We quantified the number of cells showing ~100% colocalization between both markers (i.e., total overlap; compare AP-1B+μ1B-myc in Fig. 3), cells with ~50% doubly labeled structures (i.e., partial overlap), or cells with less than ~10% of overlap between both markers (i.e., no overlap; compare AP-1A+μ1B-myc in Fig. 3). We found that AP-1A–HA and AP-1B–myc showed total or partial overlap in ~10 or ~20% of the cells, respectively. Under the same conditions, we found that AP-1B–HA and AP-1B–myc showed total overlap in nearly 90% of the cells. However, our attempts to compare AP-1–HA and AP-1B–myc staining patterns by immuno-EM failed because the labeling densities of the markers were too low to yield statistically significant data. In any event, the fluorescence data strongly suggest that there is little colocalization between AP-1A and AP-1B.

Exocyst recruitment is dependent on AP-1B expression

The mammalian exocyst complex has been implicated in basolateral targeting. The Sec6/8 subcomplex was found to localize to the lateral membrane in MDCK cells and moreover, antibodies directed against Sec6/8 inhibited the fusion of basolateral vesicles (but not apical vesicles) with the plasma membrane (Grindstaff et al., 1998). Recently, Exo70 as well as the Sec6/8 subcomplex were shown to localize to the perinuclear region of PC12 or NRK cells, respectively (Vega and Hsu, 2001; Yeaman et al., 2001).

To explore the possibility that the mammalian exocyst might be associated with the AP-1B pathway, we labeled LLC-PK1 cells stably expressing μ1A or μ1B using antibodies for endogenous Sec8 and Exo70. Both exocyst subunits were readily detected in the perinuclear region of AP-1B–expressing cells (Fig. 4 A, bottom panels). In more apical focal planes, Exo70 was also found at plasma membranes corresponding to regions of lateral cell–cell contact. In contrast, LLC-PK1 cells without μ1B failed to recruit Sec8 and Exo70 to membranes either in the Golgi region or laterally (Fig. 4 A, top panels). We quantified the extent of membrane staining in ~100 cells and found that only ~30 or ~10% of LLC-PK1::μ1A cells showed detectable membrane staining of Sec8 or Exo70, respectively. In contrast, ~90% of μ1B-expressing cells had detectable membrane staining of Sec8. The same result was found for Exo70 membrane staining in LLC-PK1::μ1B cells (Fig. 4 B). Thus, the expression of AP-1B facilitated membrane recruitment of exocyst components.

To characterize the perinuclear site at which the exocyst subunits were found, we performed a series of double-labeling experiments. Fig. 4 C illustrates that the Exo70-positive structures (green) were distinct from cisternal Golgi elements (GM130) and furin-containing regions of the TGN. However, partial overlap was observed with γ-adaptin, which denotes areas positive for both AP-1A/B. Far more striking, however, was the association of Exo70 and internalized Tfn or Tfn receptor, markers of early and recycling endosomes (Fig. 4 C). Similar results were obtained for Sec8 (not depicted).

Next, we investigated if VSVG might also appear in this Tfn-positive zone after exit from the Golgi complex. VSVG-

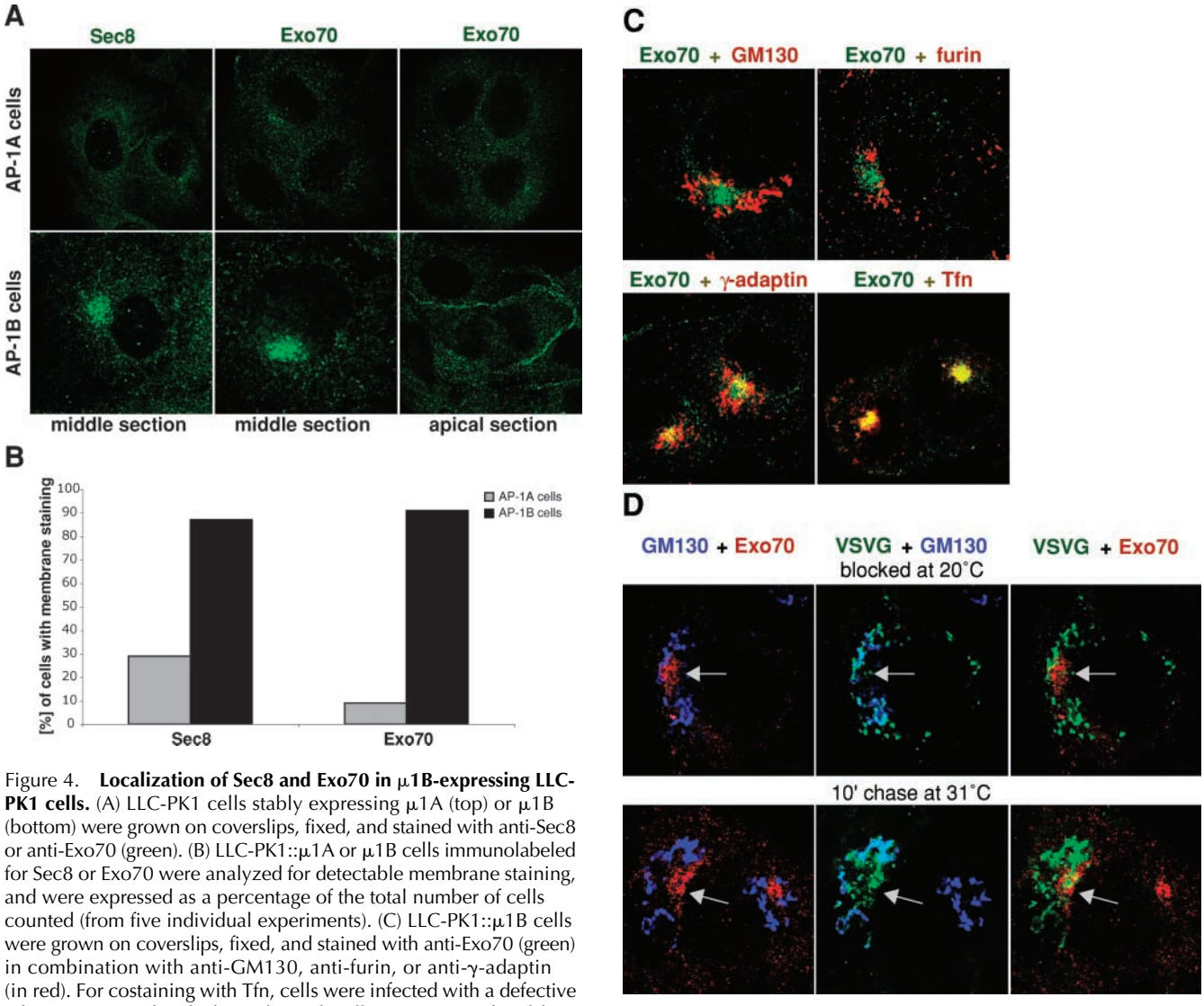

Figure 4. **Localization of Sec8 and Exo70 in μ1B-expressing LLC-PK1 cells.** (A) LLC-PK1 cells stably expressing μ1A (top) or μ1B (bottom) were grown on coverslips, fixed, and stained with anti-Sec8 or anti-Exo70 (green). (B) LLC-PK1::μ1A or μ1B cells immunolabeled for Sec8 or Exo70 were analyzed for detectable membrane staining, and were expressed as a percentage of the total number of cells counted (from five individual experiments). (C) LLC-PK1::μ1B cells were grown on coverslips, fixed, and stained with anti-Exo70 (green) in combination with anti-GM130, anti-furin, or anti-γ-adaptin (in red). For costaining with Tfn, cells were infected with a defective adenovirus encoding hTfnR. After 1 d, cells were manipulated for the uptake of Alexa® 594–labeled Tfn into recycling endosomes, fixed, and immunolabeled for Exo70 (green). (D) LLC-PK1::μ1B cells grown on coverslips were infected with defective adenoviruses encoding VSVG-ts045-GFP and incubated for 5 h at 37°C, followed by an overnight incubation at 39°C. Cells were then incubated for 2 h at 20°C and fixed directly (top panels) or chased for 10 min at 31°C (bottom panels) before fixation. Fixed cells were immunolabeled for GM130 (blue) and Exo70 (red). Arrows denote the Exo70-positive region. (A, C, and D) Specimens were analyzed by confocal microscopy, and representative merged images are shown.

ts045 was accumulated in the Golgi of AP-1B–expressing LLC-PK1 cells at 20°C and then released briefly at 31°C. As shown in Fig. 4 D, when blocked at 20°C, VSVG-ts045 (green) largely colocalized with GM130 (blue; top panels). However, within 10 min after shifting to 31°C, VSVG-ts045 became segregated from GM130-positive structures and exhibited some spatial overlap with Exo70 (red; Fig. 4 D, bottom panels). Thus, upon exit from the Golgi complex, VSVG-ts045 appeared at least partially in the Exo70-positive zone.

To directly compare the localization of Sec8 or Exo70 with AP-1B, we infected LLC-PK1::μ1A cells with a defective adenovirus encoding μ1B-myc. As shown in Fig. 5, the transient expression of μ1B-myc induced membrane recruitment of both Sec8 and Exo70. Moreover, Sec8 and Exo70 showed strong colocalization with AP-1B–myc in the perinuclear region of the large majority of cells.

Together, we demonstrated that AP-1B facilitates membrane association of at least two subunits of the exocyst complex to the perinuclear region of LLC-PK1 cells. Moreover, the recruitment was to structures that were closely associated with, or possibly identical to, Tfn-containing recycling endosomes.

AP-1A and AP-1B do not form hybrid coats

The fact that AP-1A and AP-1B labeled largely different areas of the perinuclear region and also differed in their ability to recruit exocyst components suggested that the two adaptors define distinct membrane populations. To address this possibility directly, we devised an approach to selectively isolate AP-1A– or AP-1B–containing structures by immunoisolation. For these experiments, we generated Caco-2 cell lines stably transfected with HA-tagged μ1A or μ1B cDNAs, in addition to the well-characterized LLC-PK::μ1A-HA and

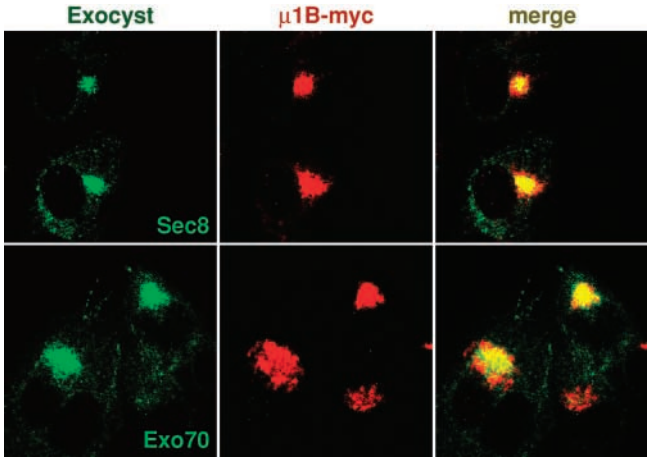

Figure 5. **AP-1B colocalizes with Sec8 and Exo70.** LLC-PK1::μ1A cells were infected with a defective adenovirus encoding μ1B-myc. After 24 h, cells were fixed and immunolabeled for μ1B-myc (red) and Sec8 or Exo70 (green). Specimens were analyzed by confocal microscopy, and representative images are shown.

μ1B-HA transfectants. Unlike LLC-PK1 cells, Caco-2 cells endogenously express both AP-1A and AP-1B complexes, facilitating the analysis by enabling us to isolate tagged AP-1A– or AP-1B–containing vesicles in cells that always make the opposite complex endogenously (Fig. 6 A). Furthermore, μ1A expression was not down-regulated in μ1A-HA–expressing Caco-2 cells, a phenomenon we previously observed in LLC-PK1 cells (Fölsch et al., 2001; also compare Fig. 6 A and the 100,000-*g* supernatant lane in Fig. 6 B).

First, we analyzed the composition of clathrin-coated structures from LLC-PK1 cells stably expressing HA-tagged μ1A or μ1B. Crude clathrin-coated vesicle pellets devoid of smooth membranes and cytosol were first isolated by centrifugation in 1% Triton X-100 (Pearse, 1982). The pellets were resuspended in a sucrose buffer and subjected to immunoisolation with anti-HA antibodies followed by SDS-PAGE and Western blotting. In both cell lines, similar amounts of clathrin adaptors were immunoprecipitated, as indicated by Western blots for clathrin heavy chain (CHC), γ-adaptin, and total μ1 proteins (Fig. 6 B; top panels, lanes 3 and 6). However, AP-1A was apparently not incorporated into AP-1B–containing coats; endogenous μ1A could not be detected in AP-1B–HA precipitates probed with an antibody that reacts with μ1A and μ1B (Fig. 6 B, right, inset), although endogenous μ1A was readily detectable in the supernatant fraction. The efficiency of the immunoprecipitations was relatively low (<1% of the input), somewhat limiting the strength of this conclusion. Interestingly, μ1B often appeared as a doublet in the 100,000-*g* pellets of crude coated vesicles (Fig. 6 B). We suspect that the top band might be a phosphorylated form of μ1B (Ghosh and Kornfeld, 2003). Because we were unable to detect a higher mol wt band of μ1A under the same conditions, these data might indicate a differential regulation of AP-1A and AP-1B by phosphorylation.

We repeated these experiments using transfected Caco-2 cell lines to determine if endogenous AP-1B was brought down together with HA-tagged AP-1A–coated membranes. As shown in Fig. 6 C (lane 3), endogenous μ1B was not coprecipitated with AP-1A–HA, indicated by probing Westerns blots with an antibody specific for μ1B. On the other hand, AP-1B–HA coprecipitated both HA-tagged and endogenous μ1B (Fig. 3 C, lane 6). Thus, despite the inefficiency of the immunoprecipitation step, there was sufficient endogenous μ1B to be detected in the resulting precipitates, but only when AP-1B–HA complexes were precipitated. Conversely, AP-1A–HA coprecipitated endogenous μ1A, as suggested by probing the AP-1A–HA precipitates with an antibody that detects both μ1A and μ1B (Fig. 6 C, lane 3). Note that we do not observe any of the presumptive phosphorylated μ1 in these experiments. This was most likely due to the fact that the probes from Caco-2 cells were run on higher percentage SDS-gels than the probes from LLC-PK1 cells.

Our experiments thus far imply that AP-1A and AP-1B do not form hybrid coat populations. The specificity and distinctiveness of the two coats was further supported by the fact that only AP-1B–containing coats coprecipitated the exocyst subunits Sec8 and Exo70. This result was obtained using both LLC-PK1 and Caco-2 cells stably expressing HA-tagged μ1A or μ1B (Fig. 6, B and C; bottom panels). Although the amounts of Sec8 and Exo70 coprecipitated were somewhat variable, they were never detected upon probing AP-1A–HA precipitates.

To analyze the biochemical features of AP-1A– or AP-1B–coated structures in a fashion that did not depend upon immunoprecipitation, we subjected the crude coated vesicle pellets to linear density gradient centrifugation. The Triton-extracted, resuspended pellets were mixed with equal amounts of OptiPrep™ and spun at 350,000 *g* for 1 h. During this time, a linear density gradient was formed, and membranes that float near the top of the gradient were separated from protein complexes and insoluble material that sedimented to the bottom fractions. Fractions were harvested from the top and analyzed by Western blot.

When pellets from LLC-PK1 cells expressing transfected μ1A were analyzed in this way, virtually all of the clathrin coat components were found in the bottom fractions, as indicated by Western blots for CHC, γ-adaptin, and μ1 (Fig. 7 A, top panels). Under the conditions used, the membranes of the Golgi complex were solubilized as expected; proteins such as GRASP65 were also recovered in the bottom fractions, most likely as aggregated material. The exocyst subunits Sec8 and Exo70 were also largely restricted to the bottom of the gradient along with the cargo molecules TfnR, CI-MPR, and furin.

The situation was dramatically different in gradients from LLC-PK1 expressing transfected μ1B (Fig. 7 A, bottom panels). A significant amount of the clathrin components found in crude coated vesicle pellets floated to the top of the gradient. This material comprised most of the components associated with AP-1B adaptors including CHC, γ-adaptin, and μ1B (detected with antibodies specific to μ1B or that detected both μ1B and μ1A). Importantly, both Sec8 and Exo70, as well as the AP-1B cargo molecule TfnR, floated with the membranes in these gradients; the AP-1A cargo molecule furin remained in the bottom fractions. A portion of the CI-MPR also floated with AP-1B components, reflecting the fact that CI-MPR (which recycles basolaterally

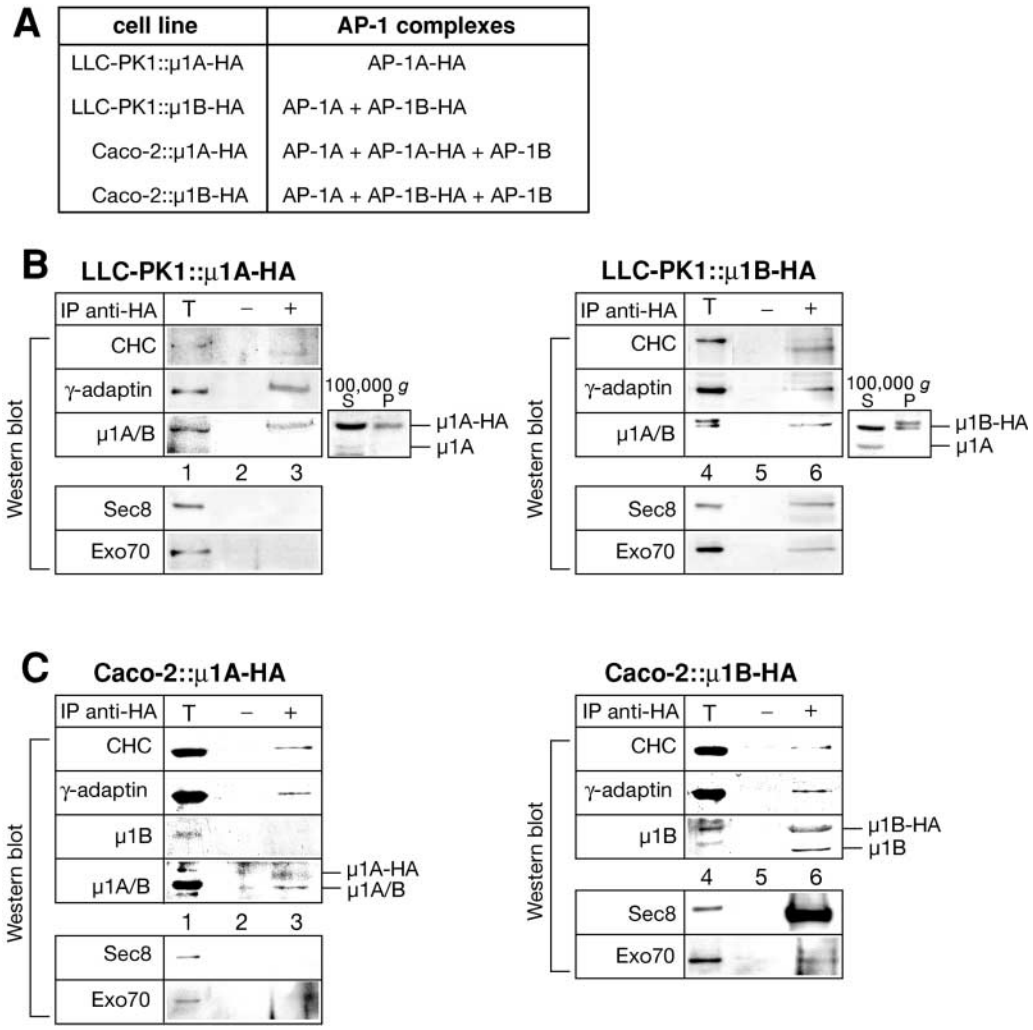

Figure 6. **Biochemical analysis of AP-1A and AP-1B vesicles.** (A) Table of used cell lines. (B) AP-1–HA coat components from LLC-PK1::μ1A-HA or μ1B-HA cells were immunoisolated using anti-HA antibodies as described in Materials and methods. Immunoprecipitates were dissolved in sample buffer and analyzed by SDS-PAGE and Western blotting using the indicated antibodies. T = 1% of the pellet fraction used for the immunoprecipitations. 100,000 *g* S and P = 0.1% of the supernatant and 1% of the pellet fractions, respectively, of the high speed spin used to obtain the crude CCV pellets. (C) AP-1–HA coat components from Caco-2 cells were isolated and analyzed as described in B. (B and C) The sample for the total input was not run directly next to the immunoprecipitation lanes, but cropped next to them after scanning of the data.

in MDCK cells) is likely to interact with AP-1B in addition to AP-1A. Because the GRASP65 was again found in the bottom fractions, the floating material is most likely not contaminated with donor membranes.

Next, we analyzed crude coated membrane pellets from Caco-2 cells in OptiPrep™ gradients (Fig. 7 B). Again, we found that AP-1B together with clathrin, Sec8 and Exo70, TfnR, and CI-MPR floated to the top. Similar results were obtained in Caco-2 cells expressing epitope-tagged μ1A or μ1B, except that μ1A was not recovered from the floating fractions (unpublished data). Unfortunately, our furin antibody did not work on Caco-2 cells and we were unable to probe Caco-2 gradients for AP-1A cargo proteins.

Finally, we asked if AP-1B components in the upper gradient fractions remained associated with each other. Fractionation was performed using crude coated vesicle pellets from μ1B-HA–expressing LLC-PK1 cells. Fractions 1–3 were collected, pooled, and AP-1B–HA was precipitated with anti-HA antibodies. As shown in Fig. 7 C, clathrin, Sec8, and Exo70 coprecipitated with AP-1B. As before, μ1B-HA ran as a double band. As a side note, the bottom doublet band runs with slightly different motility after the IP, most likely due to the presence of the antibody heavy chain running approximately at the same mol wt as μ1B-HA.

Although it is unclear why AP-1B–containing (but not AP-1A–containing) membranes floated in the gradient system used, the data nevertheless clearly emphasize that the two adaptor complexes behave in entirely distinct fashions. Thus, it would appear that AP-1A and AP-1B comprise physically and functionally distinct populations of coats and coat-associated membranes.

Discussion

Despite the clear importance of AP-1B in mediating basolateral targeting in polarized epithelial cells, a number of critical questions remain concerning its site and mechanism of action. We have provided information that helps in clarifying

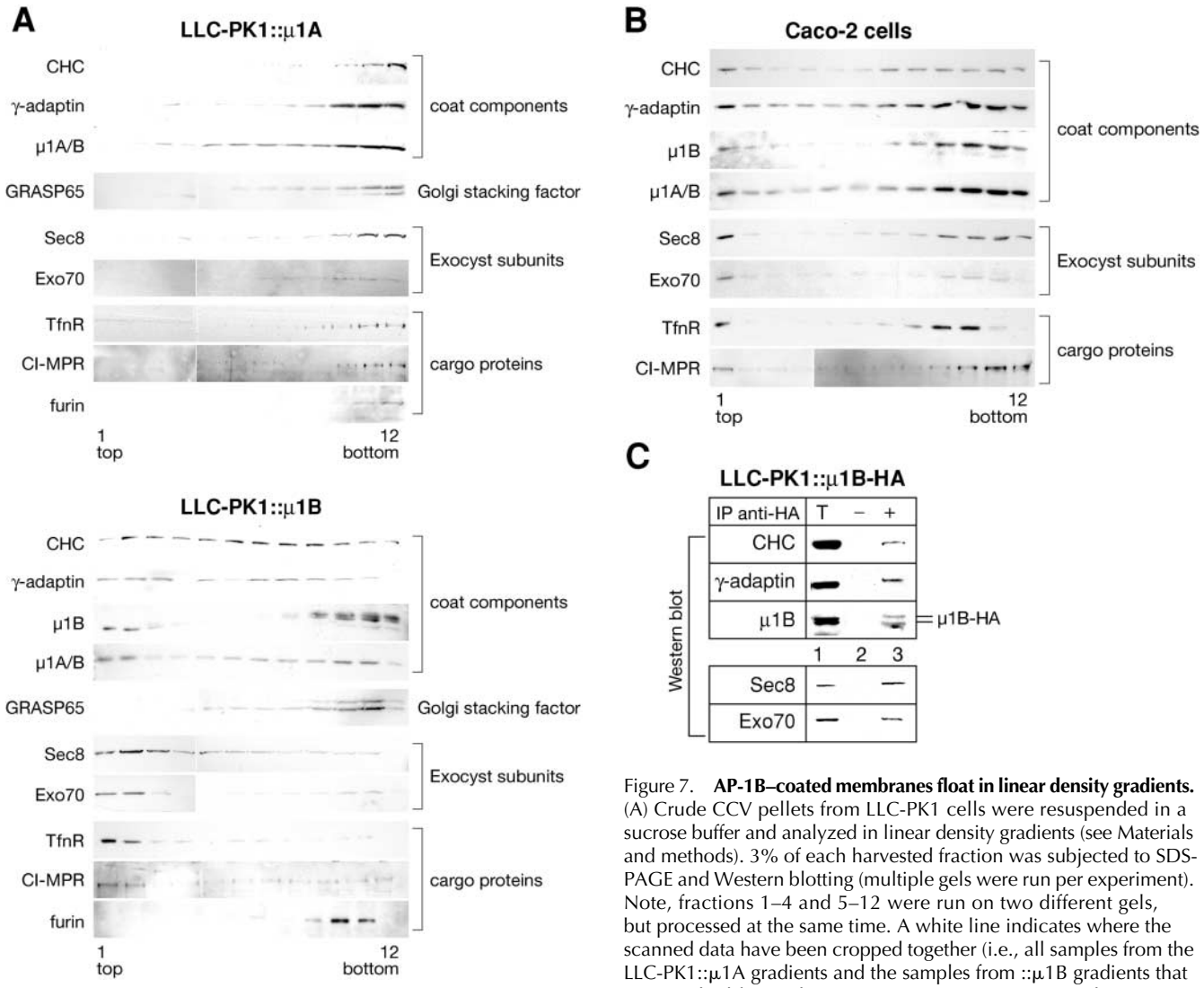

Figure 7. **AP-1B–coated membranes float in linear density gradients.** (A) Crude CCV pellets from LLC-PK1 cells were resuspended in a sucrose buffer and analyzed in linear density gradients (see Materials and methods). 3% of each harvested fraction was subjected to SDS-PAGE and Western blotting (multiple gels were run per experiment). Note, fractions 1–4 and 5–12 were run on two different gels, but processed at the same time. A white line indicates where the scanned data have been cropped together (i.e., all samples from the LLC-PK1::μ1A gradients and the samples from ::μ1B gradients that were probed for γ-adaptin, GRASP65, Sec8, Exo70, and CI-MPR). (B) Crude CCV pellets from Caco-2 cells were analyzed as described in A. Gradient samples were run on the same gel with the exception for the CI-MPR data (compare with A). (C) Crude CCV pellets from LLC-PK1::μ1B-HA cells were analyzed by density gradients as described in A. The top fractions (1–3) were harvested, pooled, and subjected to anti-HA immunoprecipitations as described in Fig. 6, A and B. T = 1% of the total pellet fraction of the initial 100,000-*g* spin.

how AP-1B function remains distinct from AP-1A despite the close relationship between the two adaptor complexes. In addition, our experiments indicate that AP-1B may act to couple the initial sorting of basolateral cargo to the recruitment of cytosolic components required for later steps of vesicle targeting or tethering at the basolateral surface.

Why are AP-1A and AP-1B vesicles different?

The observation that AP-1A and AP-1B adaptor complexes form physically and functionally distinct populations of coated membranes was unexpected, especially because they share some cargo molecules such as CI-MPR (Le Borgne et al., 1996; Meyer et al., 2000; Eskelinen et al., 2002). In addition, the two complexes differ only in a single, highly homologous subunit. However, apart from CI-MPR, AP-1A and AP-1B have nonoverlapping cargo specificities for furin, TGN38 or LDL receptor, TfnR, and VSVG. It is indeed possible that AP-1A and AP-1B form distinct coats because they recognize mostly different subsets of cargo molecules. This might be aided by different recognition of putative "docking factors" at coat assembly sites. Furthermore, assembly sites for AP-1A– and AP-1B–coated membranes might be spatially distinct, residing in different subdomains of the TGN or in entirely distinct compartments (e.g., TGN vs. some post-TGN site, perhaps recycling endosomes). For example, it could be that MPRs are incorporated into AP-1A vesicles at the TGN and into AP-1B vesicles at recycling endosomes. Our data are thus in agreement with a previous report that AP-1B can substitute for some of AP-1A's functions in μ1A-deficient fibroblasts (Eskelinen et al., 2002), but not for all cargoes (Fölsch et al., 2001).

Specificity might be enhanced by the incorporation of AP-1–associated accessory proteins, which detect the slight differences between the two complexes to ensure that hybrid vesicles do not form. The only AP-1 accessory proteins known (γ-synergin, enthoprotin/epsinR/CLINT, p56) inter-

act with the common γ subunit as opposed to the variable μ subunit (Page et al., 1999; Kalthoff et al., 2002; Wasiak et al., 2002; Hirst et al., 2003; Lui et al., 2003; Mills et al., 2003). Yet, it is conceivable that an interaction with the COOH terminus of the μ1B chain might occur. The crystal structure of the AP-2 clathrin adaptor complex has suggested that binding to lipid bilayers and a phosphorylation of the μ2 subunit may trigger a conformational change that exposes the μ2 subunit (Collins et al., 2002). Furthermore, the COOH terminus of μ2 can bind to synaptotagmin, an interaction that may serve to dock AP-2 at the plasma membrane. The interaction between AP-2/μ2 and synaptotagmin was enhanced after binding of endocytosis signals, again possibly due to conformational changes in AP-2 upon signal recognition (Haucke and De Camilli, 1999; Haucke et al., 2000).

Recently, it has been suggested that μ1A undergoes similar conformational changes concomitant with phosphorylation upon binding of AP-1A to membranes. Subsequently, the β subunit might become dephosphorylated to allow clathrin binding. In the AP-1A–binding cycle, it was further implied that the β subunit would be rephosphorylated, and thus clathrin would be released before the dephosphorylation of μ1A and the release of AP-1A into the cytoplasm (Ghosh and Kornfeld, 2003). Thus, it might be that the floating AP-1B–positive membranes in our density gradients are a population of partially uncoated vesicles. Indeed, we readily find a higher mol wt band of possibly phosphorylated μ1B, but hardly detect a similar form for μ1A in coated vesicle pellets, which might explain why we see lighter vesicle populations for AP-1B but not for AP-1A. Partial uncoating might in turn facilitate the recruitment of exocyst subunits onto AP-1B vesicles. Alternatively, the floating material might represent "break down" products of coated tubules and sorting intermediates, which form in the TGN as opposed to preformed coated vesicles (Puertollano et al., 2003; Waguri et al., 2003).

Possible links of exocyst recruitment to AP-1B pathway

There is as yet no evidence that any component of the exocyst complex interacts directly with clathrin or clathrin adaptors, thus the mechanism by which AP-1B expression results in the accumulation of Sec8 and Exo70 on AP-1B–coated membranes is unknown. It is possible that exocyst recruitment reflects interaction with an AP-1B accessory protein or some other indirect event. Future work will be aimed at elucidating the relationship of AP-1B and the mammalian exocyst complex on a molecular level.

It will also be important to determine if the action of other downstream components involved in basolateral transport may be triggered by AP-1B or exocyst recruitment. For example, in yeast, recruitment of the exocyst subunit Sec15 to secretory vesicles is regulated by the Rab GTPase Sec4p (Guo et al., 1999). One of Sec4p's closest mammalian homologues is Rab8, which has already been implicated in basolateral transport (Huber et al., 1993). We find that Rab8 is functionally linked only to the transport of AP-1B–dependent cargo in MDCK cells, and the same is true for the small GTPase Cdc42 (Ang et al., 2003). Similar considerations may also apply to the small GTPase RalA. Both Cdc42 and RalA have been suggested to play roles in basolateral targeting and/or exocyst assembly (Kroschewski et al., 1999; Brymora et al., 2001; Moskalenko et al., 2002; Sugihara et al., 2002).

The AP-1B–dependent recruitment of Sec8 and Exo70 onto membranes in the perinuclear region is in agreement with recent reports demonstrating that mammalian Sec6/8 can be found not only at presumptive fusion sites (i.e., at the lateral plasma membrane just below the junctional complexes), but also in the TGN region in epithelial-like NRK cells (Grindstaff et al., 1998; Yeaman et al., 2001). Moreover, Exo70 was shown to localize to the TGN region in PC12 cells (Vega and Hsu, 2001).

Furthermore, the unique association of Sec8 and Exo70 with AP-1B–coated membranes explains why in MDCK cells the exocyst complex is needed for LDL receptor sorting to the basolateral surface, but not for apical secretion (Grindstaff et al., 1998).

AP-1B localizes to distinct zones within the perinuclear region

It is important to note that AP-1B as well as Sec8 and Exo70 localize to perinuclear regions not identical with "classical" TGN as defined by marker proteins such as TGN38 and furin. Although AP-1A partially colocalized with TGN38 and furin (Fölsch et al., 2001; this paper), there was no colocalization between AP-1B and either of these TGN markers. However, AP-1B (but not AP-1A) was associated with basolateral VSVG on its biosynthetic pathway. Indeed, immuno-EM revealed that VSVG is sorted into clathrin-coated vesicles and buds only in the presence of AP-1B, clearly indicating that VSVG uses a different, clathrin-independent pathway to the cell surface in AP-1B minus LLC-PK1 kidney cells or fibroblasts. Classical experiments that failed to find VSVG in clathrin-coated buds of the TGN were performed in fibroblasts not likely to express AP-1B (Griffiths et al., 1985).

When released from the 20°C block, VSVG emigrated away from membranes positive for conventional Golgi to closely apposed structures that were positive for AP-1B and Exo70. Intriguingly, Exo70 also strongly localized to Tfn- and TfnR-positive recycling endosomes. Thus, it seems possible that AP-1B–dependent cargo may at least partially enter recycling endosomes before continuing to the plasma membrane after exit from the Golgi. Our data are thus in agreement with previous observations showing that Rab11 (a recycling endosome–associated GTPase) may play a role in biosynthetic traffic, at least in nonpolarized cells (Chen et al., 1998). Moreover, both the TGN and recycling endosomes are complex sorting compartments (Mellman and Warren, 2000). In the case of epithelial cells, it is also interesting to note that polarized targeting of newly synthesized and recycling glycoproteins makes use of similar or identical sorting determinants in the TGN and in the endocytic pathway (Matter et al., 1993; Aroeti and Mostov, 1994; Odorizzi and Trowbridge, 1997), probably at the level of recycling endosomes (Sheff et al., 1999). In addition, this region of the cells was previously shown to be enriched in AP-1–containing clathrin-coated endosomal structures that are accessible to internalized TfnR (Futter et al., 1998). Our immuno-EM data indicated that many of the clathrin-coated buds and tubules in the perinuclear region of LLC-PK1 cells

were positive for AP-1B. In fact, quantitative analysis revealed that most of the AP-1B–positive coated structures were found here, as opposed to being connected to morphologically identifiable Golgi elements. However, much additional work will be required to answer the question of whether VSVG actually enters TfnR-positive recycling endosomes after exit from the Golgi.

Recently, it has been suggested that AP-1B may play a role only in the recycling pathway in LLC-PK1 cells (Gan et al., 2002). However, the suggestion that basolateral cargo colocalizes with AP-1B–positive structures immediately upon exit from the Golgi complex supports a role for AP-1B in the biosynthetic pathway in addition to its role in recycling (Fölsch et al., 1999; Gan et al., 2002). Furthermore, the localization of Sec8 and Exo70 to TfnR-positive structures is in agreement with AP-1B playing a role in recycling of internalized receptors back to the basolateral surface.

Despite the fact that the precise location at which AP-1B complexes perform their functions is not yet resolved, our results clearly demonstrate the remarkable degree of specificity exhibited by AP-1B in mediating sorting and selective packaging of basolateral cargo, regardless of precisely where and when in epithelial cells these events take place. Therefore, the presented data further our understanding of how AP-1B facilitates sorting from the TGN or endosomes to the plasma membrane, a feature that is unique and cannot be mediated by any other known adaptor complex.

Materials and methods

Recombinant adenoviruses, constructs, and antibodies

Defective adenoviruses encoding VSVG-ts045 myc-GFP or its apical mutant were obtained from Kai Simons (Max Planck Institute of Molecular Cell Biology and Genetics, Dresden, Germany), and a virus encoding hTfnR was described previously (Fölsch et al., 1999).

μ1B with an internal myc tag between aa 230 and 231 was generated using PCR as described previously (Fölsch et al., 2001). The primers used for the NH_2-terminal fragment were 5′-GCGCGCGGCCGCATGTCCGCCTCGGCTGTCTTCATT-3′ and 5′-GCGCGTCGACCAAGTCTTCTTCAGAAATCAGCTTTTGTCTGATTTGTTCTGATTTGTTCTTGCTGCGGCCAGT-3′. For the COOH-terminal fragment the primers were 5′-GCGCGCGGCCGCGTGCACGTAGAGCTGGAGGATGTAAAATTC-3′ and 5′-GCGCTCGAGTAGCTGGTACGAAGTTG-3′. The construct was cloned into pBudCE4.1 (Invitrogen) and subcloned into pShuttle-CMV, and a defective adenovirus was generated as described previously (Fölsch et al., 1999).

TGN38 was amplified by PCR using TGN38-EGFP (from George Banting, University of Bristol, Bristol, UK) as template and primers 5′-CGCGCTCGAGATGCAGTTCCTGGTTGCGTTGCTCCTGCTG-3′ and 5′-CGCGTCTAGATCAAAGCTTTAGGTTCAAACGTTGGTAGTCACTGGC-3′. The PCR fragment was cloned into pShuttle-CMV.

Purchased pAbs were as follows: anti-HA (PRB-101P) from BabCo, anti-myc (sc-789) from Santa Cruz Biotechnology, Inc., anti-furin (PA1–062) from Affinity BioReagents, Inc. Purchased mAbs were as follows: anti-HA (16B12) from BabCo, anti-γ (100/3) from Sigma-Aldrich, anti-Sec8 (14) from Transduction Laboratories. pAbs against GM130, GRASP65, and TGN38 were from Graham Warren (Yale University, New Haven, CT), polyclonal anti-γ antibodies were from Margaret Robinson (University of Cambridge, Cambridge, UK), and Linton Traub (University of Pittsburgh, Pittsburgh, PA) provided polyclonal anti-μ1A/B antibodies. Suzanne Pfeffer (Stanford University, Stanford, CA) provided pAbs against the CI-MPR. mAbs against CHC (TD.1) were from Pietro deCamilli (Yale University, New Haven, CT). mAbs against Exo70 (70XI3F3) and Sec8 (ZE12) were from Shu-Chan Hsu (Rutgers University, Piscataway, NJ). pAbs specific for μ1B were as described previously (Fölsch et al., 1999). Hybridomas producing anti-hTfnR antibody (H68.4) were from American Type Culture Collection, and hybridomas producing anti-VSVG antibody (VG) were from Thomas Kreis. Secondary antibodies and Tfn labeled with Alexa® 488 or Alexa® 594 were from Molecular Probes, Inc., and Cy5-conjugated secondary antibodies were from Jackson ImmunoResearch Laboratories.

Cell culture

Stably transfected LLC-PK1 cells were maintained in α-MEM as described previously (Fölsch et al., 2001). Stably transfected Caco-2 cells were obtained as described previously (Fölsch et al., 1999), and maintained in DME containing 20% (vol/vol) FBS, 2 mM L-glutamine, 0.1 mM nonessential aa, 10 μg/ml Tfn, and 1 mg/ml geneticin.

For immunofluorescence analysis, cells were seeded on Alcian blue–treated coverslips for 3–4 d. For anti-exocyst stainings, cells were fixed in −20°C methanol for 5 min followed by a 5-min incubation at RT in PBS^{2+} (PBS plus 1.47 g/l $CaCl_2 \times 2\ H_2O$ and 1 g/l $MgCl_2 \times 6\ H_2O$). Otherwise, cells were fixed in 3% (wt/vol) PFA for 15 min at RT. Samples were blocked with 2% (vol/vol) goat serum in PBS^{2+} and permeabilized with 0.4% (wt/vol) saponin for 1 h. Antibodies were diluted into blocking solution, and staining as well as analysis of the samples was performed as described previously (Fölsch et al., 2001).

To express VSVG-ts045, corresponding cDNAs (100 μg/ml) were microinjected into LLC-PK1 cell nuclei. Cells were then incubated for 1.5 h at 39°C, followed by a 1.5-h incubation at 20°C and 10 min at 31°C in the presence of 0.1 mg/ml cycloheximide. Otherwise, cells were infected with defective adenoviruses encoding the protein and incubated at 37°C for 5 h, shifted to 39°C for 18–19 h, followed by incubation at 20°C for 2 h in medium containing 0.1 mg/ml cycloheximide. When indicated, cells were further incubated for 10 min at 31°C. Surface expression of VSVG was determined by microinjecting cDNAs into fully polarized LLC-PK1 cells (Fölsch et al., 1999). Proteins were expressed for 4 h at 31°C. Surface labeling was as described previously (Fölsch et al., 1999). Transient transfections were done using LipofectAMINE™ (Invitrogen) according to the manufacturer's protocol. Uptake of Alexa® 594–conjugated Tfn was performed as described previously (Fölsch et al., 2001).

EM

Cells were infected with defective adenoviruses encoding VSVG-ts045 myc-GFP as described previously (Fölsch et al., 1999). Infected cells were incubated at various temperatures before fixation as described above.

Fixation and preparation for immunocytochemistry was as described previously (Fölsch et al., 2001). Ultrathin cryosections were labeled with anti-HA antibody (16B12), followed by rabbit anti–mouse antibodies and 5 nm protein A–gold (Department of Cell Biology, Utrecht University, Utrecht, Netherlands). After fixation with 1% glutaraldehyde in PBS for 10 min at RT, sections were labeled with anti-myc antibody followed by 10-nm protein A–gold. Sections were infiltrated with 0.5% uranyl acetate in 1.8% methylcellulose, air-dried, and examined in an electron microscope (Tecnai 12; Philips).

For quantification, cells expressing detectable levels of VSVG-myc were photographed at a magnification of 30,000 and printed at a final magnification of 75,000. For each cell line examined and each labeling experiment, an average of 15–20 random fields were selected. Labeling density was estimated for both markers by dividing the number of gold particles over a given organelle by its membrane length. The latter was estimated by counting the number of intersections of membranes with a lattice grid with a 5-mm distance between lines. Structures were counted as clathrin-coated buds or vesicles only if they showed a clearly recognizable 20-nm-thick coat on the cytoplasmic side. Uncoated membranes included all other membranes (mostly Golgi cisternae, CGN, TGN, endosomes, and lysosomes) except ER, nuclear envelope, mitochondria, and plasma membrane.

Biochemical procedures

For immunoisolations, cells were split (1:1) into 6 × 20-cm dishes. After 2 d, cells were washed twofold with ice-cold PBS^{2+}, and were scraped off the plate with 2 ml buffer D (10 mM Hepes, 150 mM NaCl, 0.5 mM $MgCl_2$, 1× protease inhibitors [Boehringer], and 0.02% NaN_3 [wt/vol]). Cells were combined and homogenized with a cell cracker followed by a clarifying spin (at 4°C for 30 min; 13,000 rpm, Eppendorf centrifuge). Supernatants were harvested, adjusted with Triton X-100 to a final concentration of 1%, and spun for 1 h at 45,000 rpm and at 4°C (TLA 100.3, Beckman tabletop ultracentrifuge). Pellets were resuspended in 1.5 ml buffer D^+ (D plus 250 mM sucrose) and subjected to immunoprecipitation with mouse anti-HA antibodies bound to protein G beads. Samples were rotated end-over-end (at 4°C for 1 h) and washed threefold in buffer D^+. Immunoprecipitates were denatured in SDS-sample buffer, vigorously shaken (at 4°C for 20 min), boiled, and analyzed by SDS-PAGE and Western blotting.

For linear density gradients, pellets were resuspended in 4 ml buffer D^+ and mixed with equal amounts of OptiPrep™. Samples were spun for 1 h at 76,000 rpm and at 4°C (MLN-80, Beckman tabletop centrifuge), and 12 × 600-μl fractions were harvested starting from the top of the gradient and analyzed by SDS-PAGE and Western blotting. Detection of proteins

blotted onto nitrocellulose was performed using the ECL system according to the supplier's instruction (Pierce Chemical Co.).

Online supplemental material

LLC-PK1::μ1A-HA or μ1B-HA cells were seeded on coverslips and immunolabeled for CI-MPR (red) and μ1-HA (green). Specimens were analyzed by confocal microscopy and representative images are shown. Online supplemental material available at http://www.jcb.org/cgi/content/full/jcb.200309020/DC1.

We are grateful to our following colleagues for providing either invaluable antibodies, plasmids, and/or adenovirus stocks: George Banting, Shu-Chan Hsu, Suzanne Pfeffer, Margaret Robinson, Kai Simons, Linton Traub, and Graham Warren and Pietro DeCamilli. We also wish to thank Kimberly Zichichi and Melanie Ebersold for assistance in preparing the immunoelectron micrographs. We are indebted to Graham Warren for many helpful discussions and to the entire Mellman/Warren laboratory for support.

This work was funded by a grant from the National Institutes of Health (GM29765) to I. Mellman, who is a member of the Ludwig Institute for Cancer Research.

Submitted: 3 September 2003
Accepted: 23 September 2003

References

Ang, A.L., H. Fölsch, U.-M. Koivisto, and I. Mellman. 2003. The Rab8 GTPase selectively regulates AP-1B–dependent basolateral transport in polarized Madin-Darby canine kidney cells. *J. Cell Biol.* 163:339–350.

Aroeti, B., and K.E. Mostov. 1994. Polarized sorting of the polymeric immunoglobulin receptor in the exocytotic and endocytotic pathways is controlled by the same amino acids. *EMBO J.* 13:2297–2304.

Bonifacino, J.S., and E.C. Dell'Angelica. 1999. Molecular bases for the recognition of tyrosine-based sorting signals. *J. Cell Biol.* 145:923–926.

Brodsky, F.M., C.Y. Chen, C. Knuehl, M.C. Towler, and D.E. Wakeham. 2001. Biological basket weaving: formation and function of clathrin-coated vesicles. *Annu. Rev. Cell Dev. Biol.* 17:517–568.

Brymora, A., V.A. Valova, M.R. Larsen, B.D. Roufogalis, and P.J. Robinson. 2001. The brain exocyst complex interacts with RalA in a GTP-dependent manner: identification of a novel mammalian Sec3 gene and a second Sec15 gene. *J. Biol. Chem.* 276:29792–29797.

Chen, W., Y. Feng, D. Chen, and A. Wandinger-Ness. 1998. Rab11 is required for trans-golgi network-to-plasma membrane transport and a preferential target for GDP dissociation inhibitor. *Mol. Biol. Cell.* 9:3241–3257.

Collins, B.M., A.J. McCoy, H.M. Kent, P.R. Evans, and D.J. Owen. 2002. Molecular architecture and functional model of the endocytic AP2 complex. *Cell.* 109:523–535.

Doray, B., P. Ghosh, J. Griffith, H.J. Geuze, and S. Kornfeld. 2002. Cooperation of GGAs and AP-1 in packaging MPRs at the trans-Golgi network. *Science.* 297:1700–1703.

Drubin, D.G., and W.J. Nelson. 1996. Origins of cell polarity. *Cell.* 84:335–344.

Eskelinen, E.L., C. Meyer, H. Ohno, K. von Figura, and P. Schu. 2002. The polarized epithelia-specific mu 1B-adaptin complements mu 1A-deficiency in fibroblasts. *EMBO Rep.* 3:471–477.

Fölsch, H., H. Ohno, J.S. Bonifacino, and I. Mellman. 1999. A novel clathrin adaptor complex mediates basolateral targeting in polarized epithelial cells. *Cell.* 99:189–198.

Fölsch, H., M. Pypaert, P. Schu, and I. Mellman. 2001. Distribution and function of AP-1 clathrin adaptor complexes in polarized epithelial cells. *J. Cell Biol.* 152:595–606.

Futter, C.E., A. Gibson, E.H. Allchin, S. Maxwell, L.J. Ruddock, G. Odorizzi, D. Domingo, I.S. Trowbridge, and C.R. Hopkins. 1998. In polarized MDCK cells basolateral vesicles arise from clathrin-gamma-adaptin-coated domains on endosomal tubules. *J. Cell Biol.* 141:611–623.

Gan, Y., T.E. McGraw, and E. Rodriguez-Boulan. 2002. The epithelial-specific adaptor AP1B mediates post-endocytic recycling to the basolateral membrane. *Nat. Cell Biol.* 4:605–609.

Ghosh, P., and S. Kornfeld. 2003. AP-1 binding to sorting signals and release from clathrin-coated vesicles is regulated by phosphorylation. *J. Cell Biol.* 160:699–708.

Griffiths, G., S. Pfeiffer, K. Simons, and K. Matlin. 1985. Exit of newly synthesized membrane proteins from the trans cisterna of the Golgi complex to the plasma membrane. *J. Cell Biol.* 101:949–964.

Grindstaff, K.K., C. Yeaman, N. Anandasabapathy, S.C. Hsu, E. Rodriguez-Boulan, R.H. Scheller, and W.J. Nelson. 1998. Sec6/8 complex is recruited to cell-cell contacts and specifies transport vesicle delivery to the basal-lateral membrane in epithelial cells. *Cell.* 93:731–740.

Guo, W., D. Roth, C. Walch-Solimena, and P. Novick. 1999. The exocyst is an effector for Sec4p, targeting secretory vesicles to sites of exocytosis. *EMBO J.* 18:1071–1080.

Guo, W., M. Sacher, J. Barrowman, S. Ferro-Novick, and P. Novick. 2000. Protein complexes in transport vesicle targeting. *Trends Cell Biol.* 10:251–255.

Haucke, V., and P. De Camilli. 1999. AP-2 recruitment to synaptotagmin stimulated by tyrosine-based endocytic motifs. *Science.* 285:1268–1271.

Haucke, V., M.R. Wenk, E.R. Chapman, K. Farsad, and P. De Camilli. 2000. Dual interaction of synaptotagmin with mu2- and alpha-adaptin facilitates clathrin-coated pit nucleation. *EMBO J.* 19:6011–6019.

Hirst, J., and M.S. Robinson. 1998. Clathrin and adaptors. *Biochim. Biophys. Acta.* 1404:173–193.

Hirst, J., A. Motley, K. Harasaki, S.Y. Peak Chew, and M.S. Robinson. 2003. EpsinR: an ENTH domain-containing protein that interacts with AP-1. *Mol. Biol. Cell.* 14:625–641.

Huber, L.A., S. Pimplikar, R.G. Parton, H. Virta, M. Zerial, and K. Simons. 1993. Rab8, a small GTPase involved in vesicular traffic between the TGN and the basolateral plasma membrane. *J. Cell Biol.* 123:35–45.

Kalthoff, C., S. Groos, R. Kohl, S. Mahrhold, and E.J. Ungewickell. 2002. Clint: a novel clathrin-binding ENTH-domain protein at the Golgi. *Mol. Biol. Cell.* 13:4060–4073.

Keller, P., and K. Simons. 1997. Post-Golgi biosynthetic trafficking. *J. Cell Sci.* 110:3001–3009.

Kroschewski, R., A. Hall, and I. Mellman. 1999. Cdc42 controls secretory and endocytic transport to the basolateral plasma membrane of MDCK cells. *Nat. Cell Biol.* 1:8–13.

Le Borgne, R., G. Griffiths, and B. Hoflack. 1996. Mannose 6-phosphate receptors and ADP-ribosylation factors cooperate for high affinity interaction of the AP-1 Golgi assembly proteins with membranes. *J. Biol. Chem.* 271:2162–2170.

Lui, W.W., B.M. Collins, J. Hirst, A. Motley, C. Millar, P. Schu, D.J. Owen, and M.S. Robinson. 2003. Binding partners for the COOH-terminal appendage domains of the GGAs and gamma-adaptin. *Mol. Biol. Cell.* 14:2385–2398.

Marks, M.S., H. Ohno, T. Kirchhausen, and J.S. Bonifacino. 1997. Protein sorting by tyrosine-based signals: adapting to the Ys and wherefores. *Trends Cell Biol.* 7:124–128.

Matter, K., and I. Mellman. 1994. Mechanisms of cell polarity: sorting and transport in epithelial cells. *Curr. Opin. Cell Biol.* 6:545–554.

Matter, K., J.A. Whitney, E.M. Yamamoto, and I. Mellman. 1993. Common signals control low density lipoprotein receptor sorting in endosomes and the Golgi complex of MDCK cells. *Cell.* 74:1053–1064.

Mellman, I., and G. Warren. 2000. The road taken: past and future foundations of membrane traffic. *Cell.* 100:99–112.

Meyer, C., D. Zizioli, S. Lausmann, E.L. Eskelinen, J. Hamann, P. Saftig, K. von Figura, and P. Schu. 2000. μ1A-adaptin-deficient mice: lethality, loss of AP-1 binding and rerouting of mannose 6-phosphate receptors. *EMBO J.* 19:2193–2203.

Mills, I.G., G.J. Praefcke, Y. Vallis, B.J. Peter, L.E. Olesen, J.L. Gallop, P.J. Butler, P.R. Evans, and H.T. McMahon. 2003. EpsinR: an AP1/clathrin interacting protein involved in vesicle trafficking. *J. Cell Biol.* 160:213–222.

Moskalenko, S., D.O. Henry, C. Rosse, G. Mirey, J.H. Camonis, and M.A. White. 2002. The exocyst is a Ral effector complex. *Nat. Cell Biol.* 4:66–72.

Mostov, K., M.B. ter Beest, and S.J. Chapin. 1999. Catch the mu1B train to the basolateral surface. *Cell.* 99:121–122.

Odorizzi, G., and I.S. Trowbridge. 1997. Structural requirements for basolateral sorting of the human transferrin receptor in the biosynthetic and endocytic pathways of Madin-Darby canine kidney cells. *J. Cell Biol.* 137:1255–1264.

Ohno, H., J. Stewart, M.C. Fournier, H. Bosshart, I. Rhee, S. Miyatake, T. Saito, A. Gallusser, T. Kirchhausen, and J.S. Bonifacino. 1995. Interaction of tyrosine-based sorting signals with clathrin-associated proteins. *Science.* 269:1872–1875.

Ohno, H., T. Tomemori, F. Nakatsu, Y. Okazaki, R.C. Aguilar, H. Fölsch, I. Mellman, T. Saito, T. Shirasawa, and J.S. Bonifacino. 1999. Mu1B, a novel adaptor medium chain expressed in polarized epithelial cells. *FEBS Lett.* 449:215–220.

Page, L.J., P.J. Sowerby, W.W. Lui, and M.S. Robinson. 1999. Gamma-synergin: an EH domain–containing protein that interacts with gamma-adaptin. *J. Cell Biol.* 146:993–1004.

Pearse, B.M. 1982. Coated vesicles from human placenta carry ferritin, transferrin,

and immunoglobulin G. *Proc. Natl. Acad. Sci. USA.* 79:451–455.

Puertollano, R., N.N. van der Wel, L.E. Greene, E. Eisenberg, P.J. Peters, and J.S. Bonifacino. 2003. Morphology and dynamics of clathrin/GGA1-coated carriers budding from the trans-Golgi network. *Mol. Biol. Cell.* 14:1545–1557.

Robinson, M.S., and J.S. Bonifacino. 2001. Adaptor-related proteins. *Curr. Opin. Cell Biol.* 13:444–453.

Scales, S.J., R. Pepperkok, and T.E. Kreis. 1997. Visualization of ER-to-Golgi transport in living cells reveals a sequential mode of action for COPII and COPI. *Cell.* 90:1137–1148.

Sheff, D.R., E.A. Daro, M. Hull, and I. Mellman. 1999. The receptor recycling pathway contains two distinct populations of early endosomes with different sorting functions. *J. Cell Biol.* 145:123–139.

Sugihara, K., S. Asano, K. Tanaka, A. Iwamatsu, K. Okawa, and Y. Ohta. 2002. The exocyst complex binds the small GTPase RalA to mediate filopodia formation. *Nat. Cell Biol.* 4:73–78.

Thomas, D.C., C.B. Brewer, and M.G. Roth. 1993. Vesicular stomatitis virus glycoprotein contains a dominant cytoplasmic basolateral sorting signal critically dependent upon a tyrosine. *J. Biol. Chem.* 268:3313–3320.

Toomre, D., P. Keller, J. White, J.C. Olivo, and K. Simons. 1999. Dual-color visualization of trans-Golgi network to plasma membrane traffic along microtubules in living cells. *J. Cell Sci.* 112:21–33.

Vega, I.E., and S.C. Hsu. 2001. The exocyst complex associates with microtubules to mediate vesicle targeting and neurite outgrowth. *J. Neurosci.* 21: 3839–3848.

Waguri, S., F. Dewitte, R. Le Borgne, Y. Rouille, Y. Uchiyama, J.F. Dubremetz, and B. Hoflack. 2003. Visualization of TGN to endosome trafficking through fluorescently labeled MPR and AP-1 in living cells. *Mol. Biol. Cell.* 14:142–155.

Wasiak, S., V. Legendre-Guillemin, R. Puertollano, F. Blondeau, M. Girard, E. De Heuvel, D. Boismenu, A.W. Bell, J.S. Bonifacino, and P.S. McPherson. 2002. Enthoprotin: a novel clathrin-associated protein identified through subcellular proteomics. *J. Cell Biol.* 158:855–862.

Yeaman, C., K.K. Grindstaff, and W.J. Nelson. 1999. New perspectives on mechanisms involved in generating epithelial cell polarity. *Physiol. Rev.* 79:73–98.

Yeaman, C., K.K. Grindstaff, J.R. Wright, and W.J. Nelson. 2001. Sec6/8 complexes on trans-Golgi network and plasma membrane regulate late stages of exocytosis in mammalian cells. *J. Cell Biol.* 155:593–604.